JACC Vol. 24, No. 5
November 1, 1994:1398–405

Morphologic Characteristics of Lesion Formation and Time Course of Smooth Muscle Cell Proliferation in a Porcine Proliferative Restenosis Model

ANDREW J. CARTER, DO, JOHN R. LAIRD, MD, FACC, ANDREW FARB, MD, FACC,*
WILLIAM KUFS, MD, DALE C. WORTHAM, MD, FACC, RENU VIRMANI, MD, FACC*

Washington, D.C.

Objectives. This study was performed to define the evolution of lesion morphology and its relation to thrombus formation and smooth muscle cell proliferation after experimental coronary stent placement.

Background. Restenosis after percutaneous revascularization may develop because of thrombus accumulation and smooth muscle cell proliferation. In animal models of restenosis, thrombus may assume a significant role in neointimal formation by providing an absorbable matrix into which smooth muscle cells proliferate.

Methods. Twenty-eight oversized stents were placed in the coronary arteries of 23 juvenile domestic pigs. The histologic degree of vessel injury, lesion morphometry and smooth muscle cell proliferation measured by immunolocalization with a monoclonal antibody to proliferating cell nuclear antigen (PCNA) were assessed at 24 h and 7, 14 and 28 days after stent placement.

Results. The area of thrombus was minimal at 24 h ([mean ± SE] 0.44 ± 0.12 mm^2). Neointimal area at 7 days (0.72 ± 0.20 mm^2) was similar to the area of thrombus, followed by a significant increase at 14 days (3.15 ± 0.39 mm^2) and 28 days (3.30 ± 0.28 mm^2) ($p < 0.0036$, 24 h and 7 days vs. 14 and 28 days). At 14 and 28 days, neointimal thickness correlated with the histologic degree of vessel injury ($p < 0.003$). In arteries with severe injury, the increase in neointimal thickness is accounted for by replacement of the damaged media. The smooth muscle cell proliferation index was 18.6 ± 3.5% at 7 days compared with 9.6 ± 1.3% by 14 days ($p = 0.0247$) and declined to 1.1 ± 0.97% by 28 days ($p < 0.008$, 7 and 14 days vs. 28 days).

Conclusions. Early thrombus formation is minimal, and thrombus accounts for a small portion of subsequent neointimal formation. Smooth muscle cell proliferation and matrix formation are the major factors relating to neointimal formation in this proliferative model of restenosis. The evolution of neointimal formation after coronary stenting shows maximal smooth muscle cell proliferation at 7 days, with a decline to low levels by 28 days. Therefore, these data may be useful for developing effective therapies for restenosis.

(J Am Coll Cardiol 1994;24:1398–405)

Clinical restenosis, which develops in 30% to 50% of patients after successful percutaneous revascularization, is a complex and incompletely characterized response to arterial injury (1–4). Neointimal formation, which may contribute to restenosis, develops in response to injury to coronary artery lesions after percutaneous revascularization (5,6). The relative contributions of early thrombus accumulation and smooth muscle cell proliferation to neointimal formation after percutaneous transluminal coronary angioplasty are unknown.

Data from a porcine restenosis model (7,8) suggest that neointimal formation may be dependent on early thrombus volume, which then provides a matrix for smooth muscle cell proliferation. This theory emphasizes thrombus as the major determinant of the mature neointimal area in contrast to a predominance of smooth muscle cell proliferation and matrix formation with minimal contribution of early thrombus volume (8,9). However, it seems likely that elastic recoil, thrombus formation and smooth muscle cell proliferation after arterial injury act in combination to cause restenosis. Further, the arterial response from coronary intervention is most likely affected by the underlying atherosclerotic plaque morphology, the type of intervention and the extent of vessel injury (10).

The purpose of this study was to determine the relations among thrombus formation, lesion morphology and smooth muscle cell proliferation at various times after experimental coronary stent placement in the pig. We used immunohistochemical characterization of smooth muscle cell proliferation with a monoclonal antibody to proliferating cell nuclear antigen (PCNA). PCNA is a nuclear protein cofactor for DNA polymerase delta, and its presence is specific for cells undergoing replication (11). Immunolocalization of PCNA, therefore, can provide an index of cell proliferation in the intima and media of a vessel wall that correlates well with other variables of cell proliferation such as bromodeoxyuridine and thymidine incorporation (12,13). Characterization of lesion

From the Walter Reed Army Medical Center and *Armed Forces Institute of Pathology, Washington, D.C. This study was funded by the Department of Clinical Investigation, Walter Reed Army Medical Center, Washington, D.C. The views expressed in this study are the opinions of the authors and do not reflect that of the United States Army or the Department of Defense.

Manuscript received November 24, 1993; revised manuscript received April 20, 1994, accepted June 2, 1994.

Address for correspondence: Dr. Andrew J. Carter, Cardiology Service, Walter Reed Army Medical Center, Washington, DC.

0735-1097/94/$7.00

morphology and the time course of smooth muscle proliferation are important factors for comparing the porcine model with other animal models and human coronary artery repair after injury.

Methods

Animal preparation. The animal study was approved by the institutional scientific review committee and conformed to the "Position of the American Heart Association on Research Animal Use" adopted by the Association in November 1984. Twenty-three 20- to 30-kg juvenile Yorkshire pigs on a normal chow diet underwent placement of 28 premounted tantalum mesh stents (Boston Scientific Co.) in the left anterior descending or circumflex coronary artery. Animals were medicated with aspirin (650 mg) and Procardia XL (30 mg) by mouth the evening before stent placement. Intramuscular ketamine (20 mg/kg body weight) and xylazine (4 mg/kg) were used for general anesthesia. An 8F sheath was placed retrogradely in the right carotid artery. An intraarterial bolus of heparin (5,000 U) was administered. The left main coronary artery was engaged with a Judkins right 3.5 guiding catheter, which was used as a reference for stent sizing. Placement of a 3.0- or 3.5-mm diameter, 1.5-cm long, tantalum mesh stent was completed with balloon inflations at 6 and 8 atm for 30 s. Animals were allowed to recover and were returned to care facilities. All animals remained on a normal laboratory diet. The animals were returned to the research catheterization laboratory for coronary angiography at 24 h (4 animals, 6 stents), and at 7 (5 animals, 6 stents), 14 (5 animals, 6 stents) and 28 (9 animals, 10 stents) days after implantation. After completion of angiography, the animals were killed with a lethal dose of barbiturate.

Pathologic evaluation. Immediately after euthanasia the hearts were harvested, and the coronary arteries were perfusion fixed with 10% neutral buffered formalin at 60 to 80 mm Hg for 1 h through the aortic stump. The stented coronary artery segments were carefully dissected from the epicardial surface and sectioned transversely into 2-mm segments. A representative section from the midportion of the stent was embedded in plastic and cut with a carbide knife at 4 to 5 μm. The sections were stained with hematoxylin-eosin and Movat pentachrome stains. The cross-sectional area of each midstent section was measured with digital morphometry to determine area within the internal elastic lamina and the area of the residual vessel lumen. The area within the internal elastic lamina (IEL) was considered the normal lumen area. The percent area stenosis was then defined as follows: [(IEL area − Residual lumen area)/IEL area] × 100. Neointimal area was determined by subtracting the area of the residual lumen from the area within the internal elastic lamina.

The vessel injury score was determined by the method utilized by Schwartz et al. (14). In brief, the degree of injury at each wire site was assessed as follows: grade 0 = internal elastic lamina intact with media compressed; grade 1 = internal elastic lamina lacerated with media compressed; grade 2 = internal elastic lamina and media lacerated with the external elastic lamina intact; grade 3 = external elastic lamina lacerated. Neointimal thickness was measured at each wire site. The mean injury score for each arterial segment was calculated by dividing the sum of injury scores at each wire site by the total number of wires from the midstent sections. In addition to the mean injury score, the degree of stent oversizing (stent/artery ratio) was determined with quantitative angiography. At sites of deep arterial (medial) injury (grades 2 and 3), the neointimal thickness was adjusted for the loss of media by subtracting mean normal medial thickness. The mean normal medial thickness was calculated by measuring medial thickness from at least four noninjured areas of the artery and dividing the sum by the total number of sites measured within the same arterial segment.

Quantification of smooth muscle cell proliferation. Stent wires were carefully removed from adjacent tissue sections of each arterial segment. The segments were dehydrated in graded series of alcohol and embedded in paraffin, and multiple sections were cut at 4 to 5 μm. The sections were stained with monoclonal antibodies to smooth muscle specific alpha-actin and PCNA. In brief, slides were deparaffinized and pretreated with Antigen Pretreatment Solution (Biogenex) for 5 min. The slides were then incubated with 10% normal horse serum followed by incubation with mouse antihuman PCNA antibody (Dako), 1:40 dilution, for 60 min. Biotinylated horse antimouse immunoglobulin G was used as the secondary antibody, and the detection system was a Vectastain Elite ABC kit (Vector Laboratories). Slides were counterstained lightly with hematoxylin. A section of tonsil served as a positive control for each series of immunohistochemical staining for PCNA. The total number of cells and the number of PCNA-positive cells per high power field were counted from three randomly selected regions of each section. Only cells with distinct nuclear PCNA staining were considered positive. At least 50 cells/high power field were manually counted for a minimal total of 150 cells/section to derive a PCNA index (% PCNA-positive cells = Number of PCNA-positive cells/Total number of cells × 100%). Actin staining followed the same procedure as above using mouse antihuman smooth muscle–specific actin antibody from Sigma Corp. in a 1:5,000 dilution.

Quantitative angiography. Coronary angiograms were analyzed with a computer-aided quantitative analysis (ImageComm) system using the guiding catheter as a standard. The baseline and 10-min postimplantation coronary artery diameters were measured at the midstent from nonoverlapped and nonforeshortened views. The initial stent/artery ratio (midstent lumen diameter/baseline lumen diameter) was calculated from these data for each vessel to provide an estimate of stent oversizing as a measure of arterial injury.

Statistical analysis. For each of the 28 arterial segments in the study, the stent/artery ratio, mean injury score, mean neointimal thickness, neointimal area and percent area stenosis were calculated. All data are expressed as the mean value ± SE. Mean injury score, stent/artery ratio and mean intimal

JACC Vol. 24, No. 5
November 1, 1994:1398–405

Table 1. Quantitative Angiographic Characteristics of 27 Normal Pig Coronary Artery Segments at Baseline and Immediately After Oversized Stent Placement

Time	Quantitative Angiographic Characteristic		
	Prestent Lumen Diameter (mm)	Poststent Lumen Diameter (mm)	Stent/Artery Ratio
24 h (n = 6)	2.92 ± 0.17	3.65 ± 0.29	1.26 ± 0.05
7 days (n = 5)	2.96 ± 0.14	3.54 ± 0.17	1.20 ± 0.09
14 days (n = 6)	2.87 ± 0.12	3.59 ± 0.08	1.26 ± 0.03
28 days (n = 10)	2.83 ± 0.07	3.47 ± 0.07	1.23 ± 0.03

Data presented are mean value ± SE.

thickness were analyzed with linear regression to derive a slope, intercept and correlation coefficient to determine relations. Neointimal thickness at each wire site and the adjusted neointimal thickness for grades 2 and 3 injury were compared with an unpaired *t* test. Lesion morphology and PCNA score were compared at the different time intervals using analysis of variance with Scheffé *F* tests for multiple comparisons. Significance was established with $p \leq 0.05$. All statistics were calculated using Statview 4.0 (Abacus).

Results

Twenty-three pigs on a normal chow diet underwent successful implantation of 28 stents. All pigs survived for the defined study interval. In one animal with a significantly oversized stent (1.9 to 1), acute occlusive coronary thrombosis occurred after implantation and was documented by angiography on day 7. Data from this animal were excluded from analysis.

Quantitative angiography. Twenty-eight tantalum mesh stents were placed in the left anterior descending (n = 16) or left circumflex (n = 12) coronary arteries. The mean baseline vessel lumen diameter was 2.89 ± 0.06 mm and increased to 3.56 ± 0.05 mm after oversized stent placement. The mean stent/artery ratio measured at the midstent was 1.24 ± 0.02 for all vessels. The stent/artery ratio was not significantly different for vessels studied 24 h and 7, 14 and 28 days after stent injury, as shown in Table 1.

Coronary artery morphology. At 24 h after stent placement, the coronary arteries demonstrated thinning of the media with areas of medial laceration and subintimal hemorrhage associated with deep wire penetration. A small area of mural thrombus was present adjacent to the stent wires (Fig. 1A and 2). The area of thrombus was 0.44 ± 0.12 mm^2, with a percent area stenosis of 9.8% (Table 2). At 7 days an organizing fibrin thrombus was present around the stent wires, which contained smooth muscle cells with adherent inflammatory cells, neutrophils and macrophages (Fig. 1B and 3). Cells staining positive for alpha-actin were noted on the lumen surface as well as the base of the lesion in the areas of the stent wires. The neointimal area at 7 days measured 0.72 ± 0.20 mm^2, with a percent area stenosis of 11.3 ± 2.8%. Neointimal formation increased significantly by day 14, with a mean neointimal area of 3.15 ± 0.39 mm^2 ($p = 0.0036$ vs. 7-day stents). In the 14-day stents the mean neointimal thickness measured 0.39 ± 0.15 mm, with alpha-actin-positive cells circumferentially organized on the lumen surface (Fig. 1C). At the base of the neointima, in the region of the stent wires, elongated or spindle-shaped cells were haphazardly arranged that stained positive for alpha-actin. At 28 days after injury, a cellular neointima, mean thickness 0.44 ± 0.13 mm, with abundant extracellular matrix and organized alpha-actin–positive cells was present throughout the thickness of the neointima (Fig. 1D). Inflammatory cells were occasionally noted adjacent to stent wires associated with deep vessel wall penetration. The mean neointimal area (3.30 ± 0.28 mm^2) was not significantly increased compared with the 14-day arteries ($p = 0.98$). Morphometric percent area stenosis for the 28-day stent arteries was 58.4 ± 3.9% (range 44% to 84%).

Coronary artery injury and response. The mean neointimal thickness at 14 and 28 days after stent implant had good correlation with the histologic degree of injury ($r = 0.72$, $p = 0.0026$) but only a fair correlation to the angiographic degree of oversizing ($r = 0.47$, $p = 0.056$). Neointimal thickness at each wire site correlated to the degree of arterial injury, with more neointima associated with higher grades of injury (Fig. 4 and 5). By definition, grades 0 and 1 vessel injury are not associated with medial damage. We did not adjust neointimal thickness for medial replacement at these injury grades. After adjusting the neointimal thickness of grades 2 and 3 for replacement of destroyed medial wall (neointima minus normal media), the mean neointimal thickness did not differ for the grades of injury (Fig. 4). Therefore, the increased neointimal thickness at sites of deep arterial wall penetration (grades 2 and 3) was accounted for by replacement of the normal media. This is also reflected in the concentric lesions and resultant circular lumen seen in this study.

Quantification of cell proliferation. The percent of PCNA-positive cells was measured at 24 h and at 7, 14 and 28 days. The 24-h specimens did not exhibit smooth muscle cell proliferation within the media. The mural thrombus in these specimens was devoid of smooth muscle cells and lacked PCNA positivity. At 7 days after stent implantation, 18.6 ± 3.5% of cells in the neointima exhibited PCNA immunoreactivity (Fig. 6). The cell proliferation index declined by 14 days to 9.6 ± 1.34% ($p = 0.0247$ vs. 7 days) and demonstrated an even lower level of proliferation at 28 days of 1.1 ± 0.97% ($p < 0.008$, 7 and 14 days vs. 28 days). The relation of smooth muscle cell proliferation with neointimal formation is demonstrated in Figure 7.

Discussion

Animal models for the study of arterial injury and repair have improved our understanding of restenosis and have proved useful for the study of therapies designed to limit neointimal formation. However, frequently a therapy proved effective in an animal model will fail to demonstrate a clinical benefit in humans. The inconsistencies between animal and clinical trials may be explained by limitations of the models or

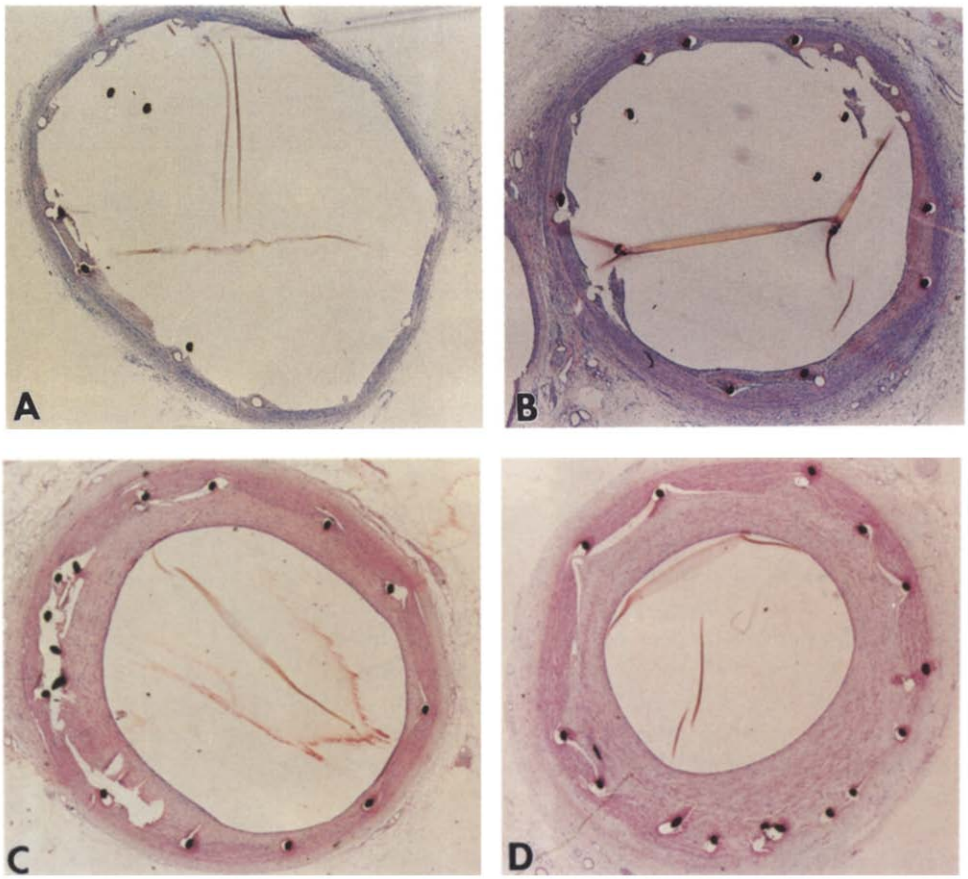

Figure 1. Photomicrographs of plastic-embedded sections of coronary artery segments at 24 h and 7, 14 and 28 days after stent placement. **A,** At 24 h, a small area of thrombus is identified. **B,** On day 7, the neointima consists of an organizing fibrin thrombus without a significant increase in area compared with that at 24 h. **C,** The neointima at 14 days exhibits smooth muscle cells circumferentially organized on the lumen surface and haphazardly arranged in the region of the stent wires. The neointimal area at 14 days has significantly increased compared with that at 24 h and 7 days. **D,** By 28 days, an organized cellular neointima with abundant extracellular matrix is present. Hematoxylin-eosin ×20, reduced by 34%.

ineffective drug dosing as well as the complex process of restenosis. In most animal models of restenosis, an intimal proliferative lesion is induced in a nonatherosclerotic vessel; it therefore is the result of wound healing from arterial injury. By contrast, a restenosis lesion after percutaneous revascularization of an atherosclerotic vessel may be the result of elastic recoil, early thrombus accumulation, smooth muscle cell proliferation and matrix formation, occurring alone or in combination. Characterization of the evolution of lesion morphology in animal models and after angioplasty in humans is necessary to better understand the pathophysiology of restenosis and to develop effective preventive strategies.

Figure 2. High power magnification of thrombus formation adjacent to a stent wire 24 h after injury. Platelets, red blood cells and inflammatory cells are entrapped in fibrin mesh. The surface of the thrombus shows platelet aggregates. Hematoxylin-eosin ×350, reduced by 26%.

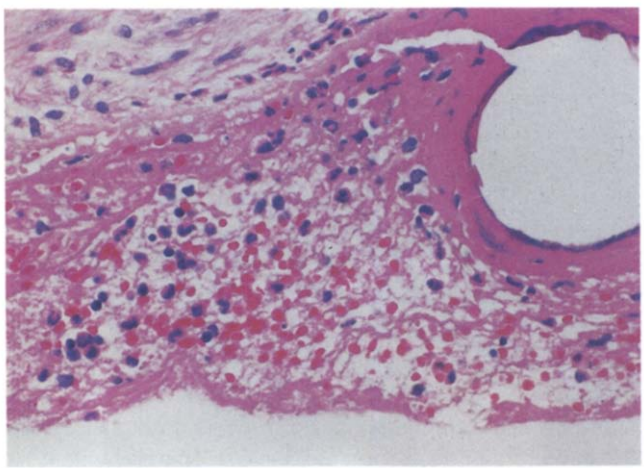

Figure 3. An organizing thrombus with scattered inflammatory cells within the thrombus and on the lumen surface is present at 7 days after stent placement. Note the presence of medial compression under the stent wire. Hematoxylin-eosin ×100, reduced by 26%.

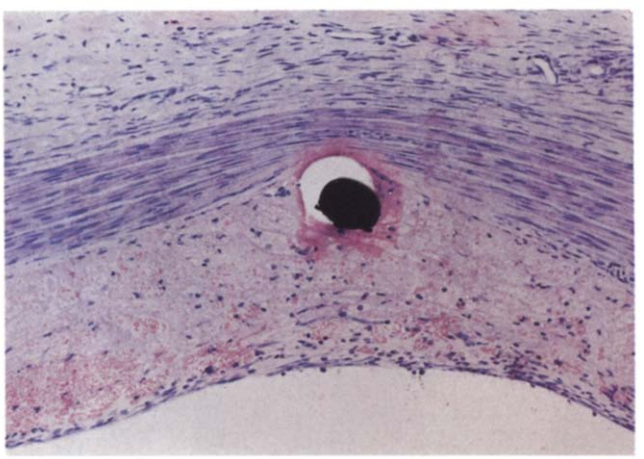

JACC Vol. 24, No. 5
November 1, 1994:1398–405

Table 2. Coronary Artery Morphologic and Injury Characteristics After Stent Placement in a Porcine Restenosis Model

Time	Histomorphologic Characteristic				
	Mean Injury Score	Internal Elastic Lamina Area (mm^2)	Residual Lumen Area (mm^2)	Neointimal Area (mm^2)	Percent Area Stenosis
24 h (n = 6)	0.74 ± 0.20	5.45 ± 0.85	5.01 ± 0.19	0.44 ± 0.12*	9.8 ± 4.2
7 days (n = 5)	0.73 ± 0.18	5.89 ± 0.88	5.17 ± 0.81	0.72 ± 0.20	11.3 ± 2.8
14 days (n = 6)	1.09 ± 0.17	5.62 ± 0.45	2.47 ± 0.67†	3.15 ± 0.39†	54.6 ± 10.5‡
28 days (n = 10)	0.76 ± 0.14	5.94 ± 0.30	2.64 ± 0.26†	3.30 ± 0.28†	58.4 ± 3.9‡

*Area of thrombus. †$p < 0.0036$ compared with 24 h and 7 days. ‡$p < 0.0018$ compared with 24 h and 7 days. Data are expressed as mean value ± SE.

The present study demonstrates that neointimal formation in response to moderately oversized coronary stent placement follows peak smooth muscle cell proliferation and does not require a large early thrombus. These data are useful for comparison with clinical restenosis and may further improve our understanding of this process.

Animal models of restenosis. In the porcine restenosis model developed by Schwartz et al. (14), neointimal proliferative lesions were induced in normal coronary arteries by injury with metal (stainless steel or tantalum) coils oversized 1.5 to 2 times the normal vessel diameter, resulting in deep arterial wall injury (mean injury score 1.9). The mean neointimal thickness at 28 days in their study was 0.72 mm. In our study, we observed less neointimal formation at 28 days (mean neointimal thickness 0.44 ± 0.14 mm) than seen in the previous studies. However, the degree of vessel injury in our study was not as severe (mean injury score 0.83, maximum 1.5). In the Schwartz et al. (14) study, the neointimal thickness was 0.41 ± 0.04 mm for vessels with an injury score of ≤1.5 (mean injury score 1.0 ± 0.1). Therefore, neointimal thickness is nearly identical when vessels with a similar injury score from these studies are compared. Additionally, in another study (15), a neointimal thickness of 0.6 mm was reported with a stent/artery ratio of 1.3:1 (15).

Figure 4. Bar graph of mean neointimal thickness **(open bars)** at each wire site for the four grades of vessel injury. The mean neointimal thickness increases with the grade of injury. The overlay graph **(cross-hatched bars)** demonstrates thickness of the neointima for grades 2 and 3 after correcting for replacement of the damaged media. The mean neointimal thickness corrected for replacement of the media is similar for each grade of injury. *Neointimal thickness minus media; p = NS compared with grades 0 and 1.

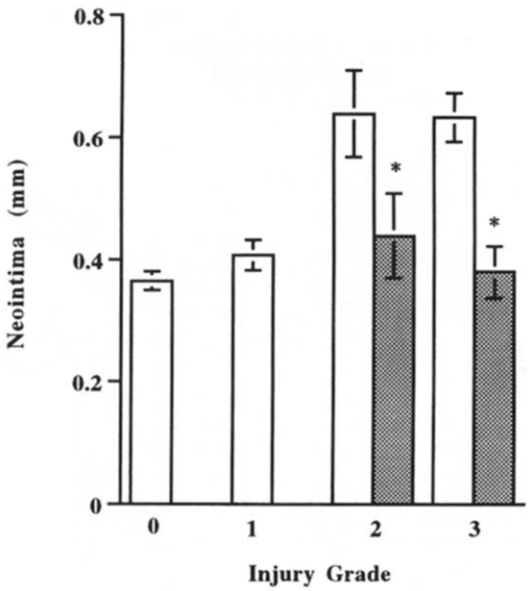

The proportional relation of vessel injury to neointimal thickness at 14 and 28 days in the present study is consistent with that in previous studies (14,16). However, we did observe more concentric lesions, with replacement of medial loss accounting for the increased neointimal thickness at sites of deep vessel penetration. This finding was not expected and may be related to differences in stent design or to a phenomenon of arterial repair to preserve a concentric lumen for laminar blood flow. In previous coronary stent studies with a coil configuration (14), the resultant neointima was more eccentric. The mesh configuration of the stent in the present study compared with a coil may cause a more even distribution of vessel injury. Other mechanical properties of the stent and the lesser degree of injury in our study may also be responsible for this finding.

The combined results of these studies support the hypothesis that neointimal formation can be consistently reproduced and correlates with the degree of vessel injury in the porcine stent restenosis model. Therefore, the model can provide a means of studying the process of arterial repair and testing therapies designed to modify neointimal proliferation. However, the limitations of the model should be considered, particularly in comparison with clinical restenosis and testing specific therapies.

Mechanisms of restenosis. Human postmortem studies (17) after percutaneous transluminal coronary angioplasty have provided insight into the mechanism of balloon dilation. However, the morphologic evolution of lesion formation after coronary angioplasty is less well defined than the immediate effects of balloon angioplasty. Angioplasty often results in laceration of the internal elastic lamina, therefore exposing deep arterial wall tissue to components of the platelet-coagulation system. Mural thrombus formation at the angioplasty site has been proposed as a mechanism for restenosis (18). Morphologic assessment of lesion formation at various times after arterial injury in animal models indicates that early mural thrombus formation may provide an absorbable matrix for smooth muscle cell proliferation (7). However, the exact

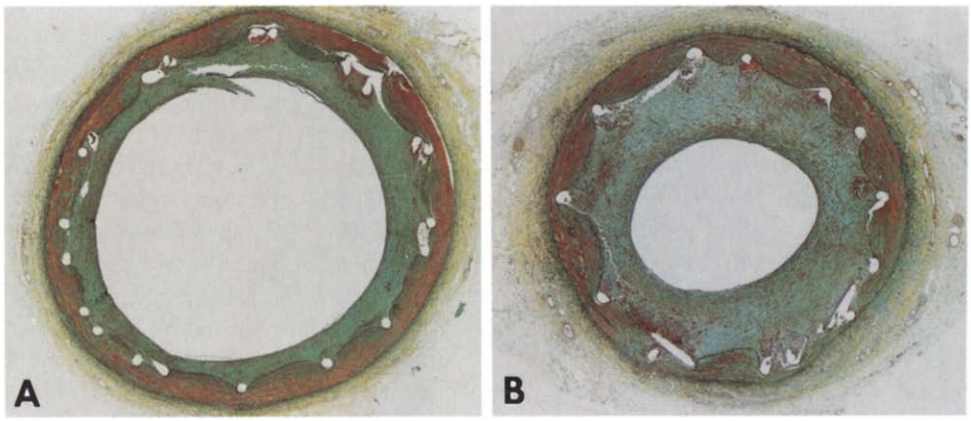

Figure 5. Movat pentachrome stains of coronary artery sections from the left circumflex (**A**) and left anterior descending (**B**) coronary arteries in the same animal 14 days after stent placement. Note the concentric lumen with greater neointimal formation in the more injured left anterior descending coronary segment (**B**). Medial destruction is evident in the lower right quadrant of segment **B**, whereas segment **A** does not have any grade 2 or 3 injury. The increased neointimal thickness in this area of the left anterior descending coronary artery is accounted for by replacement of the damaged media. ×20, reduced by 34%.

Figure 6. Photomicrographs of adjacent sections at 7 days after stent placement. **A**, Section immunostained with a monoclonal antibody to proliferating cell nuclear antigen. A significant proportion of nuclei are positive. ×300, reduced by 26%. **B**, An adjacent section stained with smooth muscle-specific alpha-actin. ×350, reduced by 26%.

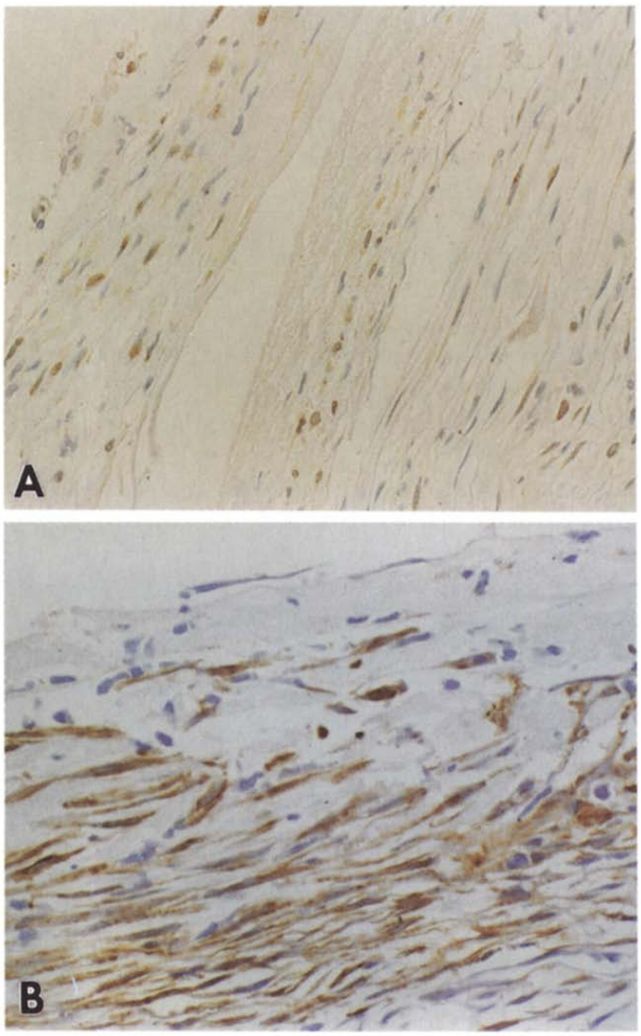

contribution of early thrombus volume to restenosis is unknown.

An alternative paradigm for restenosis was proposed on the basis of previous data from a porcine model. The morphologic assessment of lesion formation in the previous studies indicates that neointimal formation occurs in four stages (7). In stage 1, at 24 h, a large mural thrombus is present. In stage 2, 3 to 4 days, inflammatory cells infiltrate the organizing thrombus. Smooth muscle cell proliferation, primarily on the basis of cell morphology, is most evident at 7 to 9 days (stage 3). From these data, the investigators concluded that smooth muscle cells colonized the large mural thrombus, leading to neointimal formation. In contrast, in the present study, early thrombus as measured by vessel morphometry was minimal at 24 h (Table

Figure 7. Graph of neointimal area (**bars**) and percent PCNA-positive smooth muscle cells (**lines**) at 24 h and 7, 14 and 28 days after stent injury. The area of thrombus (neointimal area) is minimal at 24 h. A significant increase in neointimal area occurs from day 7 to 14, after the peak of the cell proliferation index. Low levels of cell proliferation are present at 28 days. PCNA = proliferating cell nuclear antigen.

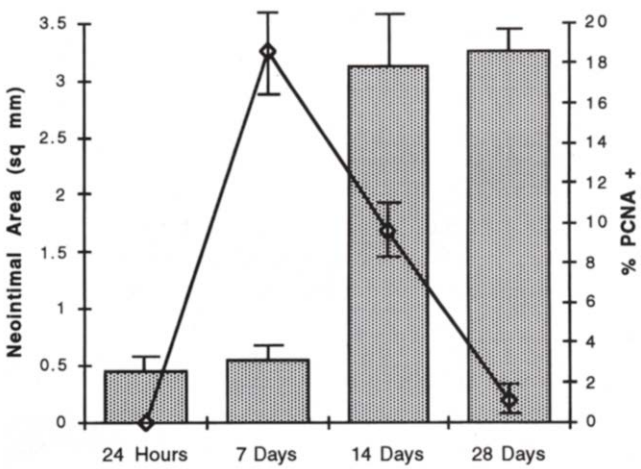

JACC Vol. 24, No. 5
November 1, 1994:1398–405

2). The area of thrombus at 24 h accounts for <15% of the neointimal area by 14 and 28 days.

The differences in the morphologic evolution of neointimal formation in the present study compared with previous studies in the porcine model are most likely related to the degree of vessel injury because similar antithrombotic and stent deployment methods were used in the studies. This theory is supported by data from a porcine carotid balloon injury model. In the study by Heras et al. (19), the degree of early thrombus accumulation was dependent on the severity of injury and the type of anticoagulation. Deep medial laceration resulted in substantially more platelet deposition, measured by indium-111–labeled platelets, than did only subendothelial injury. Together, these findings highlight significant differences present in animal models of restenosis that may be important to the testing of therapies designed to inhibit neointimal proliferation. An antithrombotic agent may significantly reduce neointimal formation in a model dependent on a large volume of thrombus, but it may be less effective in the present model.

We also studied the relation of smooth muscle cell proliferation to neointimal formation. In the present study, which was limited to 4 weeks, the process of neointimal formation was nearly complete within 2 weeks after injury. This is consistent with previous animal studies (20,21), some of which have even demonstrated lesion regression after 3 months. In our study, the interval of maximal neointimal formation was from day 7 to day 14, and this followed the peak in smooth muscle cell proliferation. The time course of smooth muscle cell proliferation in our study is consistent with that reported in other experimental models (22–25). In the atherosclerotic rabbit carotid and iliac models (22,23), peak intimal cell proliferation occurred during the first 7 days after balloon injury and declined to low levels by 28 days. In previous pathologic studies of coronary arteries from humans and in animal models after stent placement (15,26), an inflammatory or foreign body reaction has been reported that could cause prolonged smooth muscle cell proliferation, possibly by means of macrophage-derived growth factors. In our study, the cell proliferation index was only 1% by 28 days, which is similar to the proportion of PCNA-positive cells (0.85 ± 1.29%, mean ± SD) in advanced human atheroma (12). Therefore, although inflammatory cells were identified adjacent to the stent wires at 28 days after implantation, they do not appear to contribute to sustained smooth muscle cell proliferation in this model.

The morphologic evolution of lesion formation and its relation to smooth muscle cell proliferation in the present study should be compared with clinical restenosis, where angiographic studies after balloon angioplasty and intracoronary stenting (27) indicate that neointimal formation continues for at least 3 to 6 months after intervention. Recent immunohistochemical and in situ hybridization studies (28,29) of atherectomy specimens after coronary intervention have failed to demonstrate consistently high levels of cell replication or a similar early peak as in animal models. O'Brien et al. (28) reported that only 18% of primary and 26% of restenosis lesions were PCNA positive by the immunoperoxidase technique, with the majority demonstrating <1% positive cells/specimen. However, Pickering et al. (29), utilizing immunohistochemistry and in situ hybridization, showed higher levels of PCNA expression in primary (3.6% immunopositive cells) and restenosis (12.0% immunopositive cells) atherectomy specimens from active coronary and peripheral arterial lesions up to 12 months after the initial intervention. The data from these studies are inconsistent and include only a small number of specimens within the first few days after the initial procedure. The divergent results reported in these recent studies may be explained by differences in methods of tissue fixation, immunostaining and the inclusion of peripheral vascular atherectomy with coronary atherectomy specimens. Also, tissue selection bias may be present in these studies because the amount of tissue recovered with atherectomy is small, and it may be difficult to sample multiple areas of the vessel. Therefore, a comparison of cell proliferation between these recent human data and the present study would not be appropriate.

Implications for stent design. The differences in the coronary artery response to injury in our study compared with previous studies in the pig are likely related to differences in the degree of vessel injury or oversizing. However, we used a different stent design, which could account for our findings. A particular stent configuration, for example, coil versus mesh, may cause more or less arterial injury with a similar degree of oversizing. If a stent induces more arterial injury, then subsequent neointimal formation will be more extensive because of destruction of the media. In addition, other factors, such as the type and surface area of metal and radial strength of the prostheses, could influence thrombogenicity and the amount of neointimal formation. A study comparing coronary artery injury and intimal proliferation after oversized stent injury using the presently available metallic designs would be required to better understand these stent interactions with the vessel wall.

Summary. We characterized the time course of smooth muscle cell proliferation and its relation to neointimal formation in a proliferative porcine model of restenosis. Neointimal cell proliferation and matrix formation are the predominant factors contributing to lesion formation. Thrombus accounts for <15% of the mature neointimal area. The evolution of lesion formation in the present study differs from previous animal studies and from some aspects of clinical restenosis. Histomorphometric characterization of the evolution of lesion formation in animal models is essential for the appropriate design of studies that test therapies to reduce neointimal formation and to determine the relevance to restenosis.

We thank Lynn Bailey, LATG, for expert technical assistance.

References

1. Nobuyoshi M, Kimura T, Nosaka H, et al. Restenosis after successful percutaneous transluminal coronary angioplasty: serial angiographic follow-up of 229 patients. J Am Coll Cardiol 1988;12:616–23.
2. McBride W, Lange RA, Hillis LD. Restenosis after successful coronary

angioplasty: pathophysiology and prevention. N Engl J Med 1988;318: 1734–7.

3. Holmes DR, Vliestra RE, Smith HC, et al. Restenosis after percutaneous transluminal coronary angioplasty (PTCA): a report from the PTCA Registry of the National Heart, Lung, and Blood Institute. Am J Cardiol 1984;53 Suppl C:77C–81C.
4. Guiteras VP, Bourassa MG, David PR, et al. Restenosis after successful percutaneous transluminal coronary angioplasty: the Montreal Heart Institute experience. Am J Cardiol 1987;60 Suppl B:50B–5B.
5. Austin GE, Ratliff NB, Hollman J, et al. Intimal proliferation of smooth muscle cells as an explanation for recurrent coronary artery stenosis after percutaneous transluminal coronary angioplasty. J Am Coll Cardiol 1985;6: 369–75.
6. Libby P, Schwartz D, Brogi E, Tanaka H, Clinton SK. A cascade model for restenosis: a special case of atherosclerosis progression. Circulation 1992;86: Suppl III:III-47–52.
7. Schwartz RS, Holmes DR, Topol EJ. The restenosis paradigm revisited: an alternative proposal for cellular mechanisms. J Am Coll Cardiol 1992;20: 1284–93.
8. Schwartz RS, Murphy JG, Edwards WD, Camrud AR, Vlietstra RE, Holmes DR. Restenosis after balloon angioplasty: a practical proliferative model in porcine coronary arteries. Circulation 1990;82:2190–200.
9. Forrester JS, Fishbein M, Helfant R, Fagin J. A paradigm for restenosis based on cell biology: clues for the development of new preventive therapies. J Am Coll Cardiol 1991;7:758–69.
10. Farb A, Virmani R, Atkinson JB, Kolodgie FD. Plaque morphology and pathologic changes in arteries from patients dying after coronary balloon angioplasty. J Am Coll Cardiol 1990;16:1421–9.
11. Bravo R, Frank R, Blundell P, MacDonald-Bravo H. Cyclin/PCNA is the auxiliary protein of DNA polymerase-delta. Nature 1987;326:515–7.
12. Gordon D, Reidy M, Benditt E, Schwartz S. Cell proliferation in human coronary arteries. Proc Natl Acad Sci USA 1990;87:4600–4.
13. Zeymer U, Fishbein MC, Forrester JS, Cercek B. Proliferating cell nuclear antigen immunohistochemistry in rat aorta after balloon denudation: Comparison with thymidine and bromodeoxyuridine labeling. Am J Pathol 1992;141:685–90.
14. Schwartz RS, Huber KC, Murphy JG, et al. Restenosis and the proportional neointimal response to coronary artery injury: results in a porcine model. J Am Coll Cardiol 1992;19:267–74.
15. Karas SP, Gravanis MB, Santoian EC, Robinson KA, Anderberg KA, King SB. Coronary intimal proliferation after balloon injury and stenting in swine: an animal model of restenosis. J Am Coll Cardiol 1992;20:467–74.
16. Huber KC, Schwartz RS, Edwards WD, et al. Effects of angiotensin converting enzyme inhibition on neointimal proliferation in a porcine coronary injury model. Am Heart J 1993;125:695–701.
17. Kohchi K, Takebayashi S, Block PC, Hiroki T, Nobuyoshi M. Arterial changes after percutaneous transluminal coronary angioplasty: results at autopsy. J Am Coll Cardiol 1987;10:592–9.
18. Chesebro JH, Lam JYT, Badimon L, Fuster V. Restenosis after arterial angioplasty: a hemorrheologic response to injury. Am J Cardiol 1988;60: 10B–6B.
19. Heras M, Chesebro JH, Penny WJ, et al. Importance of adequate heparin dosage in arterial angioplasty in a porcine model. Circulation 1988;78:654–60.
20. Rogers GP, Minor ST, Robinson K, et al. The coronary artery response to implantation of a balloon-expandable flexible stent in the aspirin-and non-aspirin treated swine model. Am Heart J 1991;122:640–7.
21. Schatz RA, Palmaz JC, Tio FO, Garcia O, Reuter SR. Balloon-expandable intracoronary stents in the adult dog. Circulation 1987;76:450–7.
22. Hanke H, Haase KK, Hanke S, et al. Morphologic changes and smooth muscle cell proliferation after experimental excimer laser treatment. Circulation 1991;83:1380–9.
23. Clowes AW, Reidy MA, Clowes MM. Kinetics of cellular proliferation after arterial injury. Smooth muscle growth in the absence of endothelium. Lab Invest 1983;49:327–33.
24. Banai S, Shou M, Correa R, et al. Rabbit ear model of injury-induced arterial smooth muscle cell proliferation: kinetics, reproducibility, and implications. Circ Res 1991;69:748–56.
25. Hanke H, Strohschneider T, Oberhoff M, Betz E, Karsch KR. Time course of smooth muscle cell proliferation in the intima and media of arteries following experimental angioplasty. Circ Res 1990;67:6512–9.
26. van Beusekom HMM, van der Giessen WJ, van Suylen RJ, Bos E, Bosman FT, Serruys PW. Histology after stenting of human saphenous vein bypass grafts: Observations from surgically excised grafts 3 to 320 days after stent implantation. J Am Coll Cardiol 1993;21:45–54.
27. Kimura T, Nosaka H, Hiroyoshi Y, Iwabuchi M, Nobuyoshi M. Serial angiographic follow-up after Palmaz-Schatz stent implantation: comparison with conventional balloon angioplasty. J Am Coll Cardiol 1993;21:1557–63.
28. O'Brien ER, Alpers CE, Stewart DK, et al. Proliferation in primary and restenotic coronary atherectomy tissue: implications for antiproliferative therapy. Circ Res 1993;73:223–31.
29. Pickering JG, Weir L, Jekanowski J, Kearney MA, Isner JM. Proliferative activity in peripheral and coronary atherosclerotic plaque among patients undergoing percutaneous revascularization. J Clin Invest 1993;91:1469–80.